

Flexible perfect metamaterial absorber and sensor application at terahertz frequencies

E. TETIK*

Computer Education and Instructional Technology, Department of Education, Usak University, 64200, Usak, Turkey

In this study, flexible perfect metamaterial absorber at terahertz frequencies was presented. The unit cells of the proposed metamaterial have a flexible structure consisting of gold resonator, GaAs patch, polyimide substrate, and gold ground plane. First, the optimization procedure according to the geometric parameters was performed and it was shown that the permittivity and permeability parameters that determine the nature of the metamaterials were simultaneously negative for the proposed metamaterial. Then, the absorption, the reflection, and the transmission graphs of the structure were investigated. As a result, this flexible metamaterial structure had a perfect absorption with potentials to use in many applications. Finally, the pressure and permittivity sensing applications were performed for the proposed metamaterial structure. The sensing capacities of the obtained sensor structures were calculated according to the absorption results. It was seen that the proposed perfect metamaterial absorber can be used in many applications where such sensors are needed.

(Received October 4, 2019; accepted June 16, 2020)

Keywords: Metamaterial, Terahertz, Absorber, Sensor

1. Introduction

The refractive index, which is associated with the permittivity (ϵ) and permeability (μ) that determine the electromagnetic (EM) properties of the medium, is defined by the measure of bending of a light ray during passing from one medium to another. Many studies have been conducted on the refractive index concept introduced in the 1960s. However, there are limited studies on its negative values, which are listed in detail by Moroz [1]. Veselago theorized that medium can have negative refractive index according to the value of permittivity and permeability parameters at a specific frequency band [2]. Then, Pendry et al. proved that split ring resonators can have effective negative permittivity and permeability over a particular frequency region [3]. In addition, the first of these artificial materials was produced by Smith et al. and they formed a “left-handed” media ($\epsilon < 0$, $\mu < 0$) that named as metamaterial (MTM) [4]. MTMs are defined as the artificial or synthetic man-made structures that have characteristic features, unlike other materials. These features are controlled by the EM parameters such as permittivity and permeability. After the experimentally demonstration of MTMs, they attracted great attention by scientists and became an important research area that is rapidly developing. Some of these research areas can be listed as energy harvesting [5,6], sensors [7,8], chiral [9,10], antennas [11,12], flexible MTMs [13,14], MTM absorbers [15–17], and terahertz (THz) applications [18,19].

Nowadays, the production of MTMs in the THz spectrum became remarkably important. Because, there is a considerable reason to compose the innovative designs to realize applications ranging from sensors to microorganism detection, and from water MTM to solar-cell [20–24]. The THz frequency ranges (generally in the 0.1-4 THz range) correspond to a remarkable region for researches related to

MTMs. In other words, it is thought that the THz studies will overcome the lack of research between optical and mm-wave applications. Although the number of applications that can be developed using the THz technology is numerous, there are deficiencies in the design of the appropriate material type. Considering the characteristics of MTMs, it can be said that they are important candidates for the design and development of many devices such as the detectors, sensors, and filters at THz frequency range [25–27]. With the design and fabrication of the THz MTM absorber structures, the researches in this area have become crucial for researchers. Thereafter, a large number of studies have been carried out on the tunable, dual band, broadband, and multiband absorbers. The characteristic advantage of MTMs in such studies was stated as capability to determine the desired absorber results by only changes in the dimensions of the structures rather than by in the composition type.

In this paper, a flexible perfect MTM absorber structure was designed and sensor application at terahertz frequencies was realized. The proposed structure, which consists of four parts, was designed by integrating the GaAs patch and gold circle resonator on polyimide. The backside was coated with gold to obtain the perfect absorber properties. The proposed structure was optimized according to its dimension values to achieve the MTM characteristics that are the negative permittivity, permeability and refractive index. Then, the EM characteristics were obtained and the perfect absorption properties were examined. In addition, the pressure sensor application using thickness values was realized.

2. Design, brief theory and optimization

The proposed MTM absorber consists of four layers: gold ground plane, polyimide substrate, GaAs patch, and

gold circle resonator. The geometrical structure of unit cell is shown in Fig. 1a. The GaAs patches and the gold resonator form the proposed MTM absorber by sandwiching the polyimide substrate with the ground plane (Fig. 1b). Fig. 1c shows the periodic arrays (3x3) of this structure. The dimension of the resonator and ground plane determine the EM characteristic according to ϵ and μ of the perfect absorber. The proposed MTM structure is designed to have a thin and highly flexible substrate. In addition, the MTM absorber, which has a circle resonator, can be produced with easy fabrication techniques.

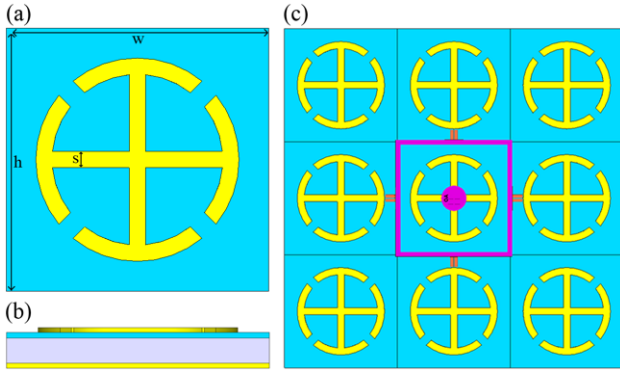


Fig. 1. The schematic structure of the proposed terahertz MTM absorber: (a) top view, (b) left view, and (c) periodical arrays (color online)

The proposed MTM structure consists of four layers – the ground plane, the polyimide substrate, the gallium arsenide (GaAs), and the resonator layers – which have $w = h = 42 \mu\text{m}$ dimensions. These layers have thickness values of 0.2, 4, 0.3, and 0.2 μm , respectively. The resonator has circular structure consisting of four gap, the inner and outer diameter of which are $b = 32.5 \mu\text{m}$ and $b = 29.9 \mu\text{m}$, respectively. In addition, the thickness of the resonator is the same as the ground plane. All resonator gaps have a 2 μm dimension. The plus shape inside the circle of resonator has $s = 2.6 \mu\text{m}$ dimension. The design and calculations of the proposed MTM absorber and sensor structures were carried out in the finite integration technique based CST Microwave Studio (Computer Simulation Technology GmbH, Darmstadt, Germany) program. The proposed structure was designed in CST Microwave Studio considering the metamaterial characteristics like the negative refractive index. The refractive index is a measure of the bending of a ray of light when passing from one medium into another. Dimensionless refractive index describing how EM radiation propagates through a medium can be defined as:

$$n = \frac{c}{v_{\text{phase}}}$$

where v_{phase} is the phase velocity of light in the medium and c is the speed of light in vacuum. Snell's Law which determines refraction of light in a material is given by the following equation:

$$n_1 \sin \theta_1 = n_2 \sin \theta_2$$

Refractive index is related to ϵ and μ according to Maxwell's equations:

$$n = \sqrt{\mu_r \epsilon_r}$$

Considering the MTM structures, it is possible to choose the negative square root in this refractive index equation. In this context, Lorentz dispersion law can state that the permittivity are dependent on frequency of light in the medium. The force (\mathbf{F}) on electrons due to electric (\mathbf{E}) and magnetic (\mathbf{B}) fields can give by the following equation:

$$\mathbf{F} = -e(\mathbf{E} + \mathbf{v} \times \mathbf{B})$$

The electron in an atom or molecule can be assumed to be bound to the equilibrium position through an elastic restoring force. In this case, if m is the mass of the electron, the equation of motion is given by,

$$m\ddot{\mathbf{r}} + m\gamma\dot{\mathbf{r}} + m\omega_0^2\mathbf{r} = -e\mathbf{E}_0e^{-i\omega t}$$

where, ω is the angular frequency of the light, ω_0 is the resonance angular frequency, and \mathbf{r} is the displacement vector. If a solution is applied according to $\mathbf{r} = \mathbf{r}_0e^{-i\omega t}$, the displacement of the electron is obtained as,

$$\mathbf{r}_0 = \frac{-e\mathbf{E}_0/m}{\omega_0^2 - \omega(\omega + i\gamma)}$$

The dipole moment due to each electron is $\mathbf{p} = -e\mathbf{r}$, and the total dipole moment per unit volume, \mathbf{P} , is expressed as the vectorial sum of all the dipoles in a unit volume. If one dipole per molecule and an average number density of N molecules per unit volume are assumed, the total dipole moment is given by,

$$\mathbf{P} = N\mathbf{p} = \frac{Ne^2\mathbf{E}/m}{\omega_0^2 - \omega(\omega + i\gamma)} = \epsilon_0\chi_e\mathbf{E}$$

where χ_e is the dielectric susceptibility. When this equation is rearranged, the dielectric permittivity is obtained as,

$$\epsilon(\omega) = 1 + \chi_e(\omega) = 1 + \frac{Ne^2/m\epsilon_0}{\omega_0^2 - \omega(\omega + i\gamma)}$$

This equation is defined as Lorentz formula for the dispersion of ϵ whose real and imaginary parts. The same results can be obtained for μ . Consider the Maxwell equations for a time-harmonic plane wave in the medium,

$$\mathbf{k} \times \mathbf{E} = \omega\mu_0\mu\mathbf{H} \text{ and } \mathbf{k} \times \mathbf{H} = -\omega\epsilon_0\epsilon\mathbf{E}$$

If $\epsilon < 0$ and $\mu < 0$, the vectors \mathbf{E} , \mathbf{H} , and \mathbf{k} form a left-handed media. But, the Poynting vector ($\mathbf{S} = \mathbf{E} \times \mathbf{H}$) remains right-handed. This is due to the fact that the Poynting vector and the wave-vector are anti-parallel. In this case, the refractive index can be expressed by the equation $\mathbf{k} = \hat{S}n\omega/c$. Since \mathbf{k} and \hat{S} are in opposite

directions, which indicates that the refractive index is negative ($n = -\sqrt{\mu_r \epsilon_r}$).

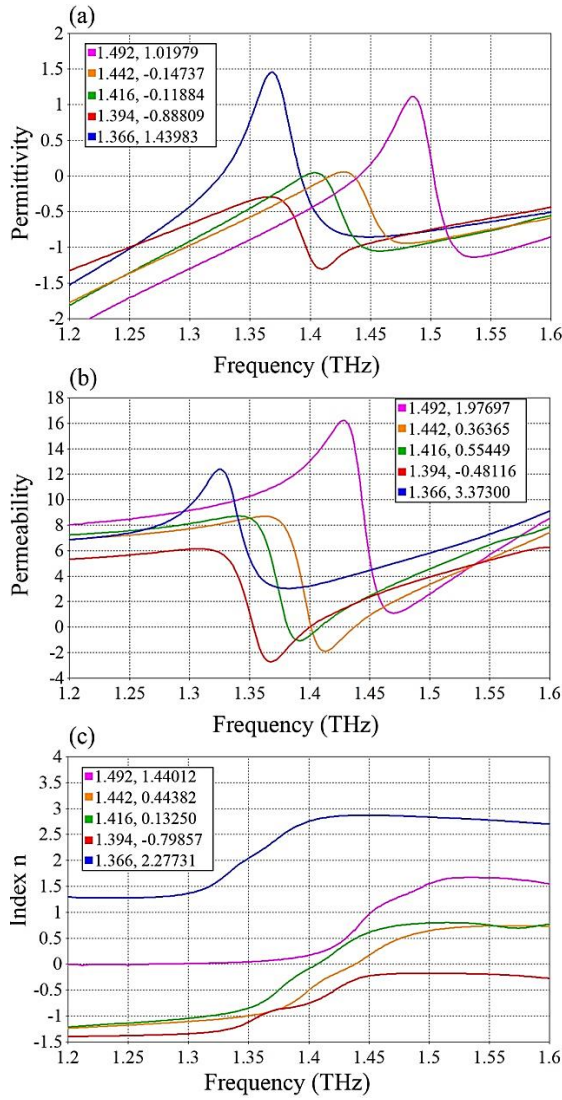


Fig. 2. The optimization results of the proposed THz MTM absorber. (a) the permittivity, (b) the permeability, and (c) the refractive index graphs for different diameter values (color online)

After the design process of the proposed structure was completed, it was performed the optimization steps of this structure. The geometric optimization stage for MTMs is remarkably important because the EM properties of the MTMs can be determined by the geometric shape and parameters. Since ϵ and μ have negative values simultaneously, it is appropriate to examine all the parameters of the structure studied as MTM. In this section, the geometric parameters of the structure proposed as MTM are investigated in detail to obtain the negative EM parameters. Fig. 2 shows the optimization results for the diameter of the resonator. It was calculated for the diameter values of 31, 31.5, 32, 32.5, and 33 μm and the ϵ , μ , and refractive index of the proposed structure were obtained in the terahertz frequency range. According to the calculation results, ϵ is positive for the diameter values of 31 and

33 μm, but was negative for 31.5, 32, and 32.5 μm values at the resonance frequency. Similarly, μ is positive for diameter values of 31, 31.5, 32, and 33 μm and only negative for 32.5 μm. The refractive index had similar results with μ and was only negative for 32.5 μm. It was understood that all of the ϵ , μ , and refractive index values were only negative for a diameter of 32.5 μm. As a result, the proposed structure demonstrated the MTM characteristics at the 1.394 THz resonance frequency. The results obtained from the optimization studies are shown in Table 1. The values in this table of the MTM structure are marked with a bold font. According to these negative values, the proposed structure shows MTM characteristics.

Table 1. The optimization results according to the diameter values of the proposed THz MTM absorber

Dia.(μm)	Freq.(THz)	ϵ	μ	Index n
31	1.492	1.019799	1.976974	1.440129
31.5	1.442	-0.14737	0.363656	0.443820
32	1.416	-0.11884	0.554496	0.132507
32.5	1.394	-0.88809	-0.48116	-0.79857
33	1.366	1.439833	3.373003	2.277317

3. Calculation method and results

MTMs can be expressed by a complex electric permittivity and magnetic permeability in an effective medium, which are formulated with $\tilde{\epsilon}(\omega) = \epsilon_1 + i\epsilon_2$ and $\tilde{\mu}(\omega) = \mu_1 + i\mu_2$, respectively. In many studies, it was aimed to obtain negative refractive structure by the real part of ϵ and μ . However, the oft-overlooked loss components of the optical parameters (ϵ_2 and μ_2), which can be used to obtain a high absorber, are considerably important research topics. Since the characteristics of MTMs are determined by permittivity and permeability, the perfect MTM absorber can be obtained by changing the effective medium properties. Therefore, the absorption coefficient of MTM structure is related to its frequency dependent transmission $T(\omega)$ and reflection $R(\omega)$, according to the formula: $A(\omega) = 1 - R(\omega) - T(\omega)$. According to the system of the MTM absorber, maximizing frequency value of the absorption $A(\omega)$ is equivalent to minimizing simultaneously both the transmission $T(\omega)$ and the reflectivity $R(\omega)$ at the same frequency range. In this context, the impedance of the MTM unit cell, which is expressed by the formula $Z(\omega) = \sqrt{\mu(\omega)/\epsilon(\omega)}$, should be matched to the free space $Z = Z_0$ for minimum reflection. On the other hand, it was provided that the imaginary part of the refractive index should be maximum to enlarge the absorption of incident waves. Thus, it seems that MMA structures can exhibit a high absorption over a narrow frequency range.

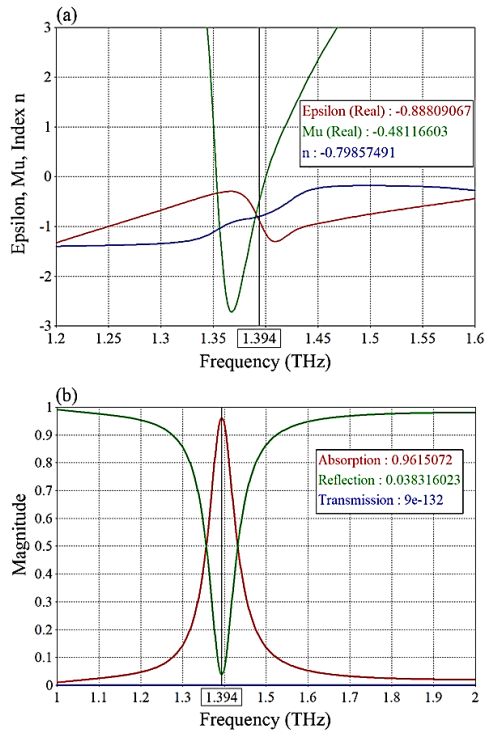


Fig. 3. (a) The real permittivity, real permeability, and refractive index graph. (b) The absorption, reflection and, transmission graphs (color online)

With the optimization procedures, the equilibrium parameters of the proposed MTM structure were obtained. The graphs of the real ϵ , real μ , and refractive index of equilibrium structure is given in Fig.3a. It has -0.88809067, -0.48116603, and -0.79857491 values at the 1.394 THz resonance frequency, respectively. Then, the absorption, reflection, and transmission results of the proposed MTM were obtained by using these equilibrium parameters. The graphs of these results are demonstrated in Fig. 3b. These indicated that the transmission was zero at the all frequency values, the reflection only has a minimum value that was 3.831 %, and the absorption which was of about 96.15 % reached its maximum value at the resonance frequency. It was seen that the proposed MTM had perfect absorption and could be used in numerous applications where absorption is important.

4. Pressure and permittivity sensing

In this section, the pressure sensor application of the proposed MTM absorber was performed at the resonance frequency. The proposed sensor architecture was constructed using a sensor layer sandwiched between the polyimide substrate, and the GaAs structures. This sensor layer was independent from the other layers and consisted of the air gap. In this way, the flexibility characteristics of the proposed sensor structure have not been affected negatively and it could be used in many sensor applications to achieve the properties that vary according to environmental changes such as pressure. The sensor layer of this structure was examined according to different gap

thicknesses. With the proper adjustment of this application, the pressure level could be changed depending on the air gap. The pressure sensing process could be performed by monitoring the separation distance between the polyimide and the GaAs layers. Considering that the thickness of one side of the proposed structure could be changed under different pressure values, the thickness of air gap would decrease when the pressure value increased. The lower the pressure value, the higher the distance between the polyimide and GaAs layers. Thus, the high and low pressures refer to narrow and wide air gaps, respectively. The obtained absorption results according to the air gap are given in Fig. 4.

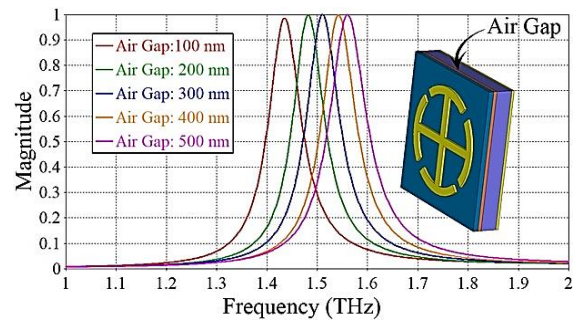


Fig. 4. The absorption graph according to the air gap values of the proposed MTM sensor structure (color online)

The air gap thickness between the polyimide and the GaAs layers was changed from 100 nm to 500 nm with 100 nm steps to realize the calculations at the THz frequency range. The proposed sensor structure has 1.4344, 1.4820, 1.5105, 1.5420, and 1.5601 THz frequency values corresponding to the gap thickness of 100, 200, 300, 400, and 500 nm, respectively. The first remarkable detail in these results, as the thickness of the gap increases, the resonance frequency of the structure shifted to higher frequencies and at the same time its magnitude value also increased. This increase revealed the perfect THz MTM absorber structure with a 99.9% absorption value. In this context, the proposed MTM absorber sensor can be used in areas where the high sensitivity and accuracy are required.

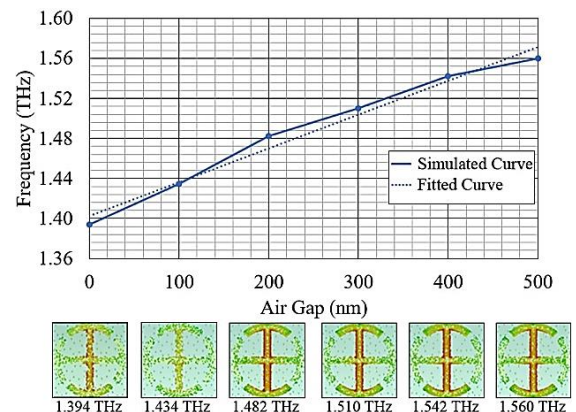


Fig. 5. The simulated and fitted curve according to the air gap values, and the surface current distribution for the air gap (color online)

To investigate the physical mechanism of the sensor applications for the proposed structure, the air gap-frequency and electric field distribution were calculated at the resonance frequency. The graphs of the obtained data are demonstrated in Fig. 5. It was seen that the proposed sensor structure appeared to have an approximately linear graph when the pressure/thickness changes. As the pressure applied to the MTM sensor increases, the thickness of the sensor layer and resonance frequency decreases. Therefore, when the thickness of the sensor layer decreases, the EM signal travels a shorter path in the proposed sensor structure and a positive shift occurs at its resonance frequency. In addition, it was obtained the surface current distributions for six MTM structures. The first one did not have a sensor layer, the other 5 structures had sensor layers of different thicknesses. The surface current distribution for the 100 nm sensor layer was reduced. However, as the thickness of the sensor layer have increased, the surface current distribution density also increased. The surface current of the proposed structure without the sensor layer had a value of 110.162 dB(A/m) at the 1.394 THz resonance frequency. When the sensor layers were added for thicknesses of 100, 200, 300, 400, and 500 nm; 108.155, 109.897, 110.326, 110.213, and 110.436 dB(A/m) of the surface current values were observed, respectively.

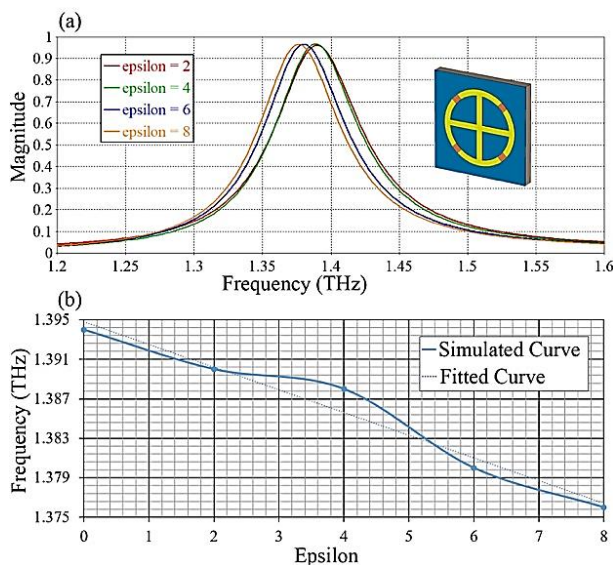


Fig. 6. (a) The absorption graph according to the ϵ values of the proposed MTM sensor. (b) The simulated and fitted curve according to the ϵ values (color online)

At the next stage, the permittivity sensing behaviors of the proposed MTM structure were investigated. The medium to be used for the permittivity sensing was placed in the four resonator gaps in the structure. The permittivity values of the inserted medium was increased from 2 to 8 with 2 steps. The absorption results of these permittivity values is demonstrated in Fig. 6a. The proposed structure had 1.39, 1.388, 1.380, and 1.376 THz frequency values corresponding to the permittivity values of 2, 4, 6, and 8, respectively. In addition, the absorption frequency values corresponding to different permeabilities are plotted in Fig.

6b. The obtained graphs showed that the absorption values of the proposed MTM structure decreased while the permittivity of the inserted medium increased from 2 to 8. The Fig. 6b shows differences in the frequency shift, but considering the fitted curve, the permeability increases can be considered to be approximately linear.

5. Conclusion

In this study, the perfect THz MTM absorber which has a flexible structure was designed at terahertz frequencies. Since the MTMs require simultaneously negative permittivity and permeability, firstly, the optimization process according to the geometric parameters of the proposed MTM structure was carried out. As a result of the calculation, it was shown that the permittivity, permeability, and refractive index was negative. Then, the absorption, the reflection and, the transmission graphs of the proposed structure were obtained. The proposed MTM structure had an absorption value of 96.15 % at the 1.394 THz resonance frequency. In this context, it showed the perfect absorber characteristics and can be used in many applications such as the sensor, superlens, energy harvesting, cloaking, and so on. Finally, the sensor application was performed for the pressure and permittivity sensing. An air layer was integrated into the proposed structure for this application, which was changed from 100 nm to 500 nm with 100 nm steps for the pressure sensor. The absorption graph of the integrated MTM structure was obtained according to air gap values. In addition, it was demonstrated that as the thickness of the range increased, the resonance frequency of the proposed structure shifted to higher frequencies. In the second stage, the permittivity sensing application was realized for the proposed MTM structure. For this, it was placed the medium used for the permittivity sensing in the four resonator gaps of the proposed structure. The permittivity values of the inserted medium changed from 2 to 8 with 2 steps. According to the results obtained, it was showed that the absorption values of the proposed structure decreased while the permittivity values of the inserted medium increased. According to the overall results, the proposed MTM structure can be used in the many sensor applications such as the pressure and permittivity sensing.

References

- [1] A. Moroz, Some negative refractive index material headlines long before Veselago work and going back as far as to 1905, (2009).
- [2] V. G. Veselago, Sov. Phys. Uspekhi **10**, 509 (1968).
- [3] J. B. Pendry, A. J. Holden, D. J. Robbins, W. J. Stewart, IEEE Trans. Microw. Theory Tech. **47**, 2075 (1999).
- [4] D. R. Smith, W. J. Padilla, D. C. Vier, S. C. Nemat-Nasser, S. Schultz, Phys. Rev. Lett. **84**, 4184 (2000).

- [5] M. Karaaslan, M. Bağmancı, E. Ünal, O. Akgol, O. Altıntaş, C. Sabah, *Opt. Quantum Electron.* **50**, 225 (2018).
- [6] H. T. Zhong, X. X. Yang, C. Tan, K. Yu, *Appl. Phys. Lett.* **109**, 253904 (2016).
- [7] E. Unal, F. Dincer, E. Tetik, M. Karaaslan, M. Bakir, C. Sabah, *J. Mater. Sci. Mater. Electron.* **26**, 9735 (2015).
- [8] X. Chen, W. Fan, C. Song, *Carbon* **133**, 416 (2018).
- [9] M. Z. Yaqoob, A. Ghaffar, I. Shakir, M. Y. Naz, S. Ahmed, Q. A. Naqvi, *Optoelectron. Adv. Mat.* **8**, 488 (2014).
- [10] Y Cheng, W Li, X Mao, *Progress In Electromagnetics Research* **165**, 35 (2019).
- [11] E. Tetik, G. D. Tetik, *Celal Bayar University Journal of Science* **14**, 1 (2018).
- [12] T. R. Muthu, A. Thenmozhi, *J. Optoelectron. Adv. M.* **20**, 486 (2018).
- [13] X. Zhao, K. Fan, J. Zhang, H. R. Seren, G. D. Metcalfe, M. Wraback, R. D. Averitt, X. Zhang, *A Phys.* **231**, 74 (2015).
- [14] K. Iwaszczuk, A.C. Strikwerda, K. Fan, X. Zhang, R. D. Averitt, P.U. Jepsen, *Opt. Express.* **20**, 635 (2012).
- [15] T. Tan, Z. Yan, H. Zou, K. Ma, F. Liu, L. Zhao, Z. Peng, *Applied Energy* **254**, 113717 (2019).
- [16] G. Sen, M. Kumar, S.N. Islam, S. Das, *Waves in Random Media* **29**, 153 (2019).
- [17] N. Muhammad, X. Tang, F. Tao, L. Qiang, O. Zhengbiao, *Materials Science and Engineering B* **249**, 114419 (2019).
- [18] A. Elakkiya, S. Radha, E. Manikandan, B. S. Sreeja, *J. Optoelectron. Adv. M.* **21**, 450 (2019).
- [19] B. Fang, Y. Chen, X. Jing, *J. Optoelectron. Adv. M.* **20**, 371 (2018).
- [20] M. Bakır, M. Karaaslan, F. Dincer, K. Delihacioglu, C. Sabah, *J. Mater. Sci. Mater. Electron.* **27**, 12091 (2016).
- [21] S. J. Park, J. T. Hong, S. J. Choi, H. S. Kim, W. K. Park, S. T. Han, J. Y. Park, S. Lee, D. S. Kim, Y. H. Ahn, *Sci. Rep.* **4**, 4988 (2014).
- [22] M. Bağmancı, M. Karaaslan, E. Ünal, O. Akgol, C. Sabah, *Opt. Quantum Electron.* **49**, 257 (2017).
- [23] B. Mulla, C. Sabah, *Plasmonics.* **11**, 1313 (2016).
- [24] J. Xie, W. Zhu, I.D. Rukhlenko, F. Xiao, C. He, J. Geng, X. Liang, R. Jin, M. Premaratne, *Opt. Express.* **26**, 5052 (2018).
- [25] C. Belacel, Y. Todorov, S. Barbieri, D. Gacemi, I. Favero, C. Sirtori, *Nat. Commun.* **8**, 1 (2017).
- [26] J. Yang, C. Gong, L. Sun, P. Chen, L. Lin, W. Liu, *Sci. Rep.* **6**, 1 (2016).
- [27] I. Al-Naib, *J. Infrared, Millimeter, Terahertz Waves* **39**, 1 (2018).

*Corresponding author: erkan.tetik@usak.edu.tr